Bull. Mater. Sci., Vol. 31, No. 2, April 2008, pp. 109–113. © Indian Academy of Sciences.

Comparative study of Co, Cr and Al-doped $LiMnO_2$ prepared by ion exchange

XIAN MING WU*, RUN XIU LI, SHANG CHEN, ZE QIANG HE and MING FEI XU†

College of Chemistry and Chemical Engineering, Jishou University, Jishou Hunan, 416000, PR China
†College of Metallurgical Science and Engineering, Central South University, Changsha 410083, PR China

MS received 5 October 2007; revised 4 January 2008

Abstract. **The Co, Cr and Al-doped $LiMnO_2$ powders were prepared by ion exchange. Phase identification, surface morphology and electrochemical properties were studied by X-ray diffraction, scanning electron microscopy and galvanostatic charge–discharge experiments. The results show that the doped $LiMnO_2$ keeps the structure of $LiMnO_2$. As compared to $LiMnO_2$, Co, Cr and Al-doped $LiMnO_2$ offers higher discharge capacity and better cycling performance. The discharge capacities of Co, Cr and Al-doped $LiMnO_2$ decreases yet the cycling performance improves with the increase of doping concentration. For these doped $LiMnO_2$ at the same doping concentration, Cr-doping shows the highest discharge capacity and best cycling performance, Al-doping offers the lowest discharge capacity and Co-doping shows the worst cycling performance.**

Keywords. **Lithium ion; doping; electrochemistry.**

1. Introduction

Orthorhombic and monoclinic $LiMnO_2$ polymorphs have gained increasing attention due to their higher realizable energy density. One significant drawback of the manganese compounds is that they are difficult to synthesize in the layered $NaFeO_2$ structure, which is common to $LiCoO_2$ and $LiNiO_2$.

Monoclinic $LiMnO_2$ (*m*-$LiMnO_2$) with layer structure is of metastable structure between rhombus and spinel. $LiMnO_2$ synthesized under equilibrium conditions is always orthorhombic $LiMnO_2$ (*o*-$LiMnO_2$) with space group, *Pmmn* (Ceder and Mishra 1999). Therefore, *m*-$LiMnO_2$ can only be prepared by the method that is thermodynamically unstable but dynamically stable.

Since *m*-$LiMnO_2$ was successfully prepared through ion exchange by Armstrong in 1996 (Armstrong and Bruce 1996), this material has drawn great attention (Guo *et al* 2002; Hwang *et al* 2002; Eriksson and Doeff 2003; Kim *et al* 2003; Lee *et al* 2003; Park *et al* 2004; Julien *et al* 2006; Myung *et al* 2006). However, the material shows relatively large capacity loss in cycling, which greatly limits its commercial application. In order to improve the performance of this material, Co, Cr and Al-doped $LiMnO_2$ was prepared and comparatively studied in this paper.

2. Experimental

Stoichiometric amount of Na_2CO_3 was added into solution of $Mn(CH_3COO)_2$ and $Co(CH_3COO)_2$ mixture, $Mn(CH_3COO)_2$ and CrC_2O_4 mixture, $Mn(CH_3COO)_2$ and $Al(CH_3COO)_3$ mixture with constant stirring to prepare $LiMnO_2$, Co, Cr and Al-doped $LiMnO_2$ precursor solution. After the solution was heated at 120°C for 3 h followed by heating at 250°C in air for 4 h, the product was grounded and then annealed at 710°C for 2 h to obtain $NaMnO_2$ and $NaM_xMn_{1-x}O_2$ (M = Cr, Co, Al). After $NaMnO_2$, $NaM_xMn_{1-x}O_2$ were added into LiBr *n*-hexanol solution of 4 mol·L^{-1} (The molar ratio of LiBr to $NaMnO_2$ is 8 : 1 to ensure the completion of ion exchange). The mixture was circumfluenced at 145–154°C for 8 h and then cooled to room temperature. After the mixture was filtered, the precipitate was washed with *n*-hexanol and ethanol followed by drying to obtain $LiMnO_2$, Co, Cr and Al-doped $LiMnO_2$ powders.

Phase identification and surface morphology of the prepared powders were studied by X-ray diffractometer (XRD) and scanning electron microscopy. Least squares method was employed to determine crystal parameter. Electrochemical measurements were conducted through a coin type cell (CR2025) with lithium metal as both counter and reference electrodes and 1 mol L^{-1} $LiPF_6$/EC (ethylene carbonate)–DMC(dimethyl carbonate) solution as electrolyte. Composite cathodes were fabricated as follows: $LiMnO_2$ or $LiMn_{1-x}M_xO_2$ (M = Cr, Co, Al), carbon black and polyvinylidene fluoride (PVDF) in the molar ratio of 80 : 12 : 8 were mixed in *n*-methyl pyrrolidone followed by a vacuum drying at 120°C for 12 h. The entire cell was assembled in an argon-filled glove box. Galvanostatic charge–discharge experiments were conducted at the discharge rate of 0·15 C between 4·5 V and 2·5 V.

*Author for correspondence (xianmingwu@163.com)

3. Results and discussion

The X-ray diffraction patterns of $NaMnO_2$ and $LiMnO_2$ are shown in figure 1. As observed in the figure, the prepared $LiMnO_2$ is of monoclinic crystal with a space group of $C2/m$. However, there are a few weak impure diffraction peaks with an intensity of less than 5%. Least squares method shows that the crystal parameters of the prepared $LiMnO_2$ are a = 5·4385 Å, b = 2·8086 Å, c = 5·3987 Å and β = 115·89°, which is very close to the values reported elsewhere (Captiaine *et al* 1996).

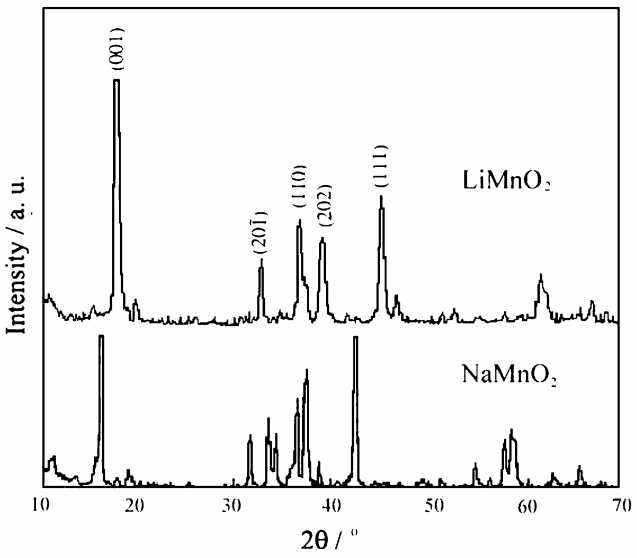

Figure 1. XRD patterns of $NaMnO_2$ and $LiMnO_2$.

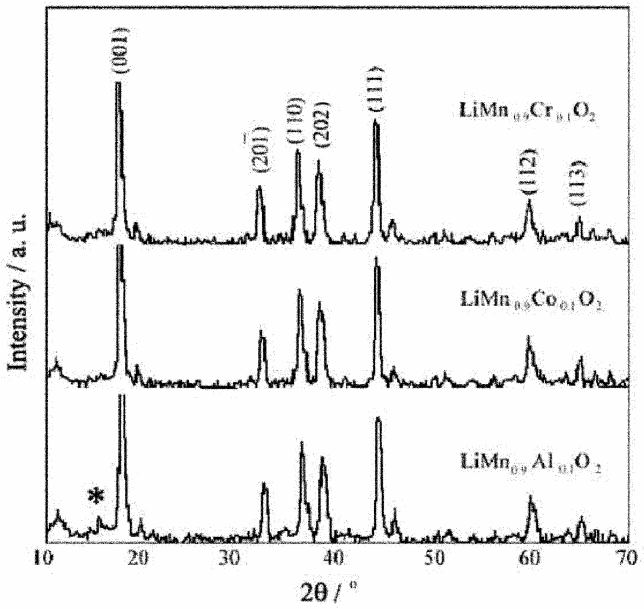

Figure 2. XRD patterns of Co, Cr and Al-doped $LiMnO_2$ (The peak with asterisk belongs to o-$LiMnO_2$).

The X-ray diffraction patterns of Co, Cr and Al-doped $LiMnO_2$ at the doping concentration of 0·05 are displayed in figure 2. As seen in the figure, all the patterns of the doped $LiMnO_2$ are similar to the undoped one. Unlike Cr-doped $LiMnO_2$ prepared by solid state reaction (Guo *et al* 2002), no impure phase can be observed in $LiMn_{0.95}Cr_{0.05}O_2$ and $LiMn_{0.95}Co_{0.05}O_2$. However, weak o-$LiMnO_2$ peak appears in the patterns of $LiMn_{0.95}Al_{0.05}O_2$. This means that a small amount of impure phase is formed in Al-doped $LiMnO_2$.

Table 1 displays the crystal parameters of $LiMnO_2$, Co, Cr and Al-doped $LiMnO_2$ at different doping concentrations. As seen in the table, the crystal parameter of doped $LiMnO_2$ is generally smaller than the undoped $LiMnO_2$. In ab plane, the shrinkage along a axis is bigger than along b axis. This means that the distortion of monoclinic crystal $LiMnO_2$ takes place after being doped, which is caused by the distortion of oxgen octahedron. For $LiMn_{1-x}M_xO_2$ at x = 0·05, Al-doping has the highest shrinkage degree, Co the second and Cr the least. This is because Cr^{3+} has the highest radius (0·615 Å), Co (0·545 Å) the second, and Al^{3+} (0·535 Å) the least. The table also shows that the crystal parameter decreases with increase in doping concentration. Cr decreases most and Al the least.

The scanning electron micrographs of $LiMnO_2$ and $LiMn_{0.95}M_{0.05}O_2$ (M = Cr, Co, Al) are presented in figure 3. As displayed in the figure, $LiMnO_2$ is of layer structure with particle size between 1 and 3 μm. Although all the doped $LiMnO_2$ with some differences keeps the structure of $LiMnO_2$, their surface is different from $LiMnO_2$. The surface of $LiMn_{0.95}Cr_{0.05}O_2$ is coarse, $LiMn_{0.95}Al_{0.05}O_2$ has a loose surface while the surface of $LiMn_{0.95}Co_{0.05}O_2$ is smooth.

The first discharge curves of $LiMnO_2$ and $LiMn_{0.95}M_{0.05}O_2$ (M = Co, Cr, Al) are displayed in figure 4. As shown in the figure, all the discharge curves show two voltage plateaus at about 3·8 V and 3 V. However, the plateaus of $LiMn_{0.95}M_{0.05}O_2$ are much more obvious than $LiMnO_2$. For these doped $LiMnO_2$, $LiMn_{0.95}Co_{0.05}O_2$ shows the highest 3·8 V plateau, $LiMn_{0.95}Al_{0.05}O_2$ the second and $LiMn_{0.95}Cr_{0.05}O_2$ the least. For the 3 V plateau,

Table 1. Crystal parameters of $LiMnO_2$ and Co, Cr and Al-doped $LiMnO_2$.

Samples	a (Å)	b (Å)	c (Å)	β
m-$LiMnO_2$	5·4385	2·8086	5·3987	115·89°
$LiMn_{0.95}Al_{0.05}O_2$	5·4183	2·8003	5·3824	115·673°
$LiMn_{0.90}Al_{0.10}O_2$	5·4152	2·8028	5·3831	115·768°
$LiMn_{0.85}Al_{0.15}O_2$	5·4134	2·8041	5·3850	115·826°
$LiMn_{0.95}Cr_{0.05}O_2$	5·4309	2·8064	5·3856	115·962°
$LiMn_{0.90}Cr_{0.10}O_2$	5·4031	2·8161	5·3746	115·604°
$LiMn_{0.85}Cr_{0.15}O_2$	5·3853	2·8227	5·3724	115·437°
$LiMn_{0.95}Co_{0.05}O_2$	5·4216	2·8027	5·3831	115·735°
$LiMn_{0.90}Co_{0.10}O_2$	5·4194	2·8001	5·3823	115·576°
$LiMn_{0.15}Co_{0.15}O_2$	5·4172	2·7989	5·3817	115·438°

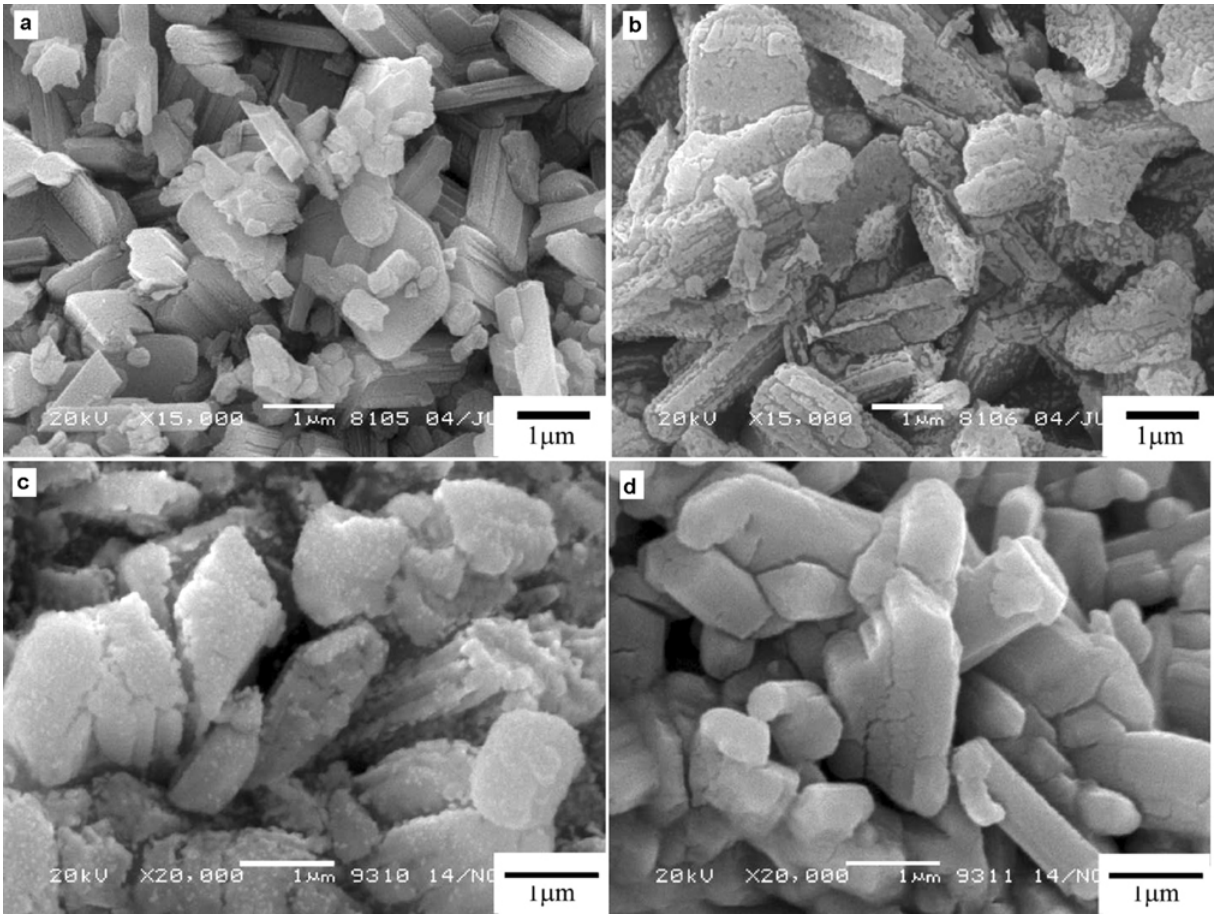

Figure 3. Scanning electron micrographs of $LiMnO_2$ and doped $LiMnO_2$: (**a**) $LiMnO_2$, (**b**) $LiMn_{0.95}Cr_{0.05}O_2$, (**c**) $LiMn_{0.95}Al_{0.05}O_2$ and (**d**) $LiMn_{0.95}Co_{0.05}O_2$.

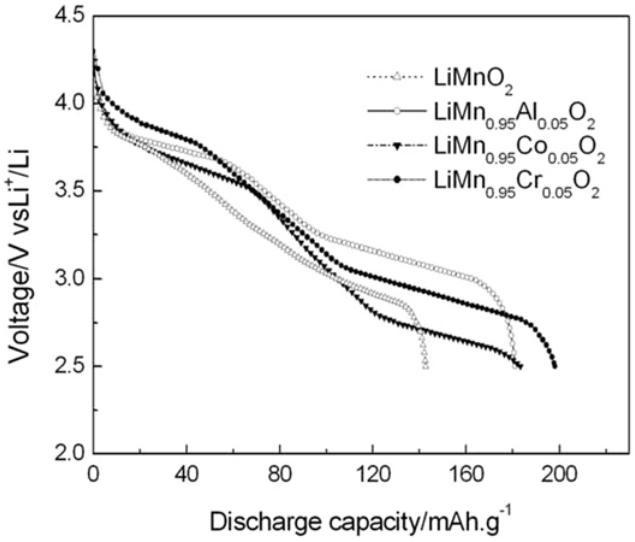

Figure 4. The first discharge curves of $LiMnO_2$ and $LiMn_{0.95}M_{0.05}O_2$ (M = Co, Cr, Al).

$LiMn_{0.95}Al_{0.05}O_2$ shows the highest plateau, $LiMn_{0.95}Cr_{0.05}O_2$ the second and $LiMn_{0.95}Co_{0.05}O_2$ the least. The figure also shows that $LiMn_{0.95}Cr_{0.05}O_2$ has the highest discharge capacity, $LiMn_{0.95}Co_{0.05}O_2$ and $LiMn_{0.95}Al_{0.05}O_2$ have almost the same discharge capacities. All doped $LiMnO_2$ shows higher discharge capacity than the undoped $LiMnO_2$.

The first discharge curves of Cr-doped $LiMnO_2$ at different doping concentrations are presented in figure 5. As observed in the figure, the discharge curves of these samples at an voltage of over 3·75 V are almost superposed. However, the discharge curves below 3·75 V are quite different. The higher the doping concentration, the lower 3 V voltage plateau will be. The figure also shows that the first discharge capacity decreases with increase in doping concentration. Same phenomena are observed for Al and Co-doped $LiMnO_2$.

The discharge curves of $LiMn_{0.95}Cr_{0.05}O_2$ cycled at different times are shown in figure 6. As seen in the figure, as the cycle number increases, the 3·8 V voltage plateau becomes longer and the two plateaus in the discharge curves become obvious. However, the 3 V voltage plateau and the discharge capacity decrease with the increase in cycle number.

The variation of discharge capacity as a function of cycle for $LiMnO_2$, Co, Cr and Al-doped $LiMnO_2$ at different doping concentrations are displayed in figure 7.

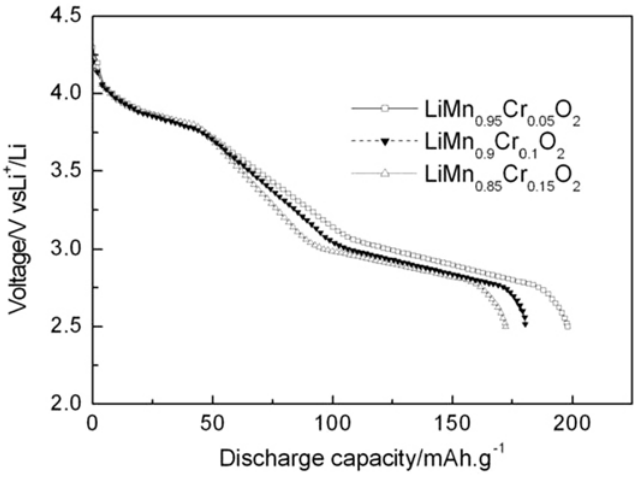

Figure 5. The first discharge curves of $LiMn_{1-x}Cr_xO_2$ at different doping concentrations.

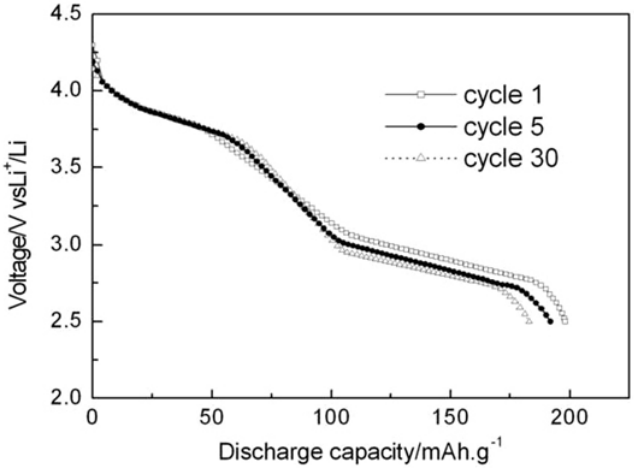

Figure 6. The discharge curves of $LiMn_{0.95}Cr_{0.05}O_2$ at different cycles.

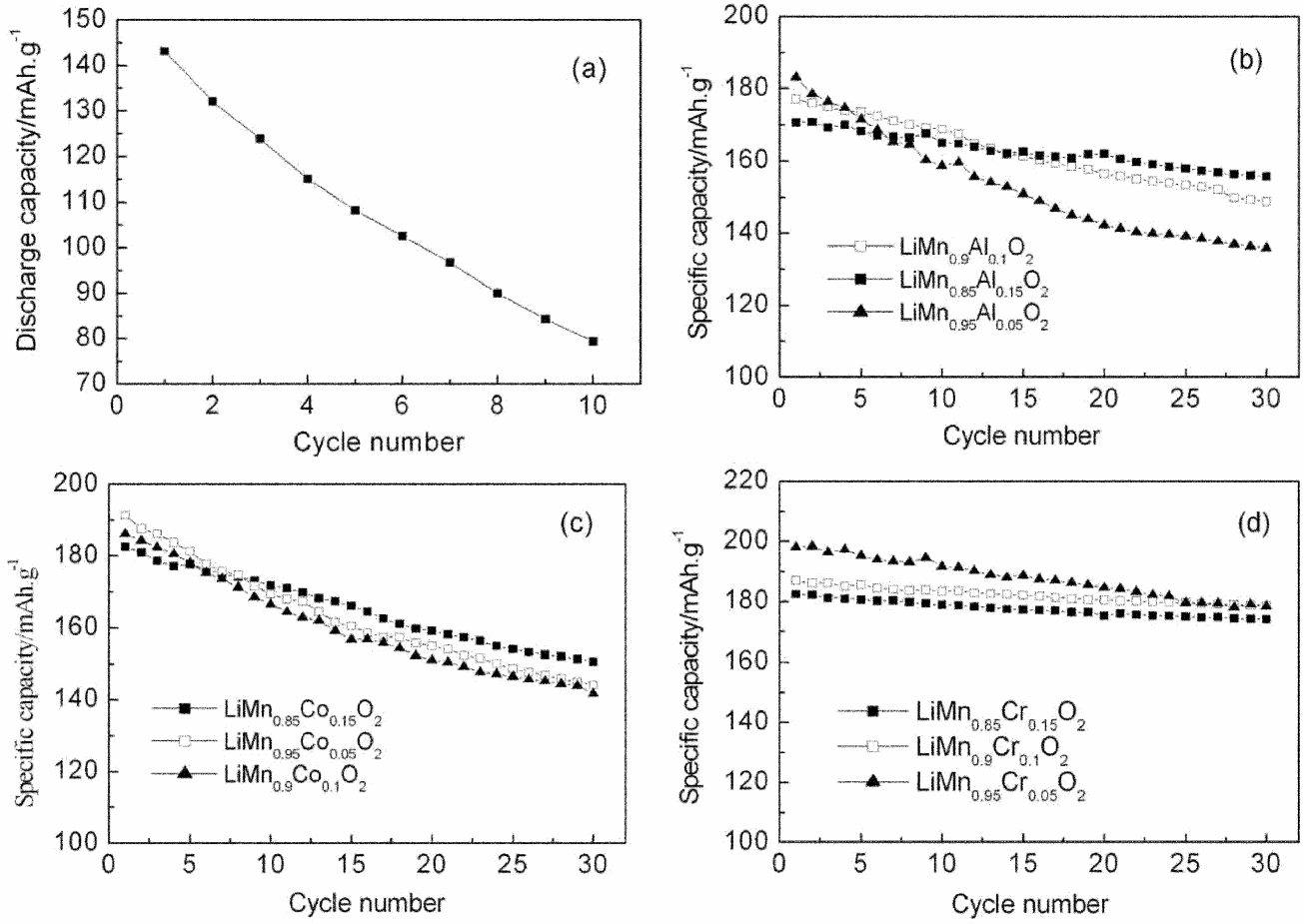

Figure 7. Cycling performance of $LiMnO_2$ and doped $LiMnO_2$: (a) $LiMnO_2$, (b) $LiMn_{1-x}Al_xO_2$, (c) $LiMn_{1-x}Co_xO_2$ and (d) $LiMn_{1-x}Cr_xO_2$.

The discharge capacity of $LiMnO_2$ decreases to less than 80 mAh·g^{-1} after 10 cycles, indicating that its cycling performance is bad. However, the doped $LiMnO_2$ show much better cycling performance than the undoped one. Among these doped $LiMnO_2$, $LiMn_{0.9}Cr_{0.1}O_2$ shows the best cycling performance with a capacity loss of 7·6 mAh·g^{-1} after 30 cycles. The discharge capacity of $LiMn_{1-x}Cr_xO_2$ is higher and the cycling performance are much better than that derived from other preparation routes (Guo *et al* 2002; Myung *et al* 2003; Gu *et al*

2004). The figure also shows that all the discharge capacities of the doped $LiMnO_2$ decreases while the cycling performance improves with the increase of doping concentration. When doping at the same doping concentration, Cr-doping shows the highest discharge capacity and best cycling performance, Al-doping shows the lowest discharge capacity and Co doping shows the worst cycling performance.

4. Conclusions

The powders of Co, Cr and Al-doped $LiMnO_2$ prepared by ion exchange technique have the structure of $LiMnO_2$. As compared to $LiMnO_2$, Co, Cr and Al-doped $LiMnO_2$ shows higher discharge capacity and better cycling performance. All the discharge capacities of Co, Cr and Al-doped $LiMnO_2$ decreases while the cycling performance improves with the increase of doping concentration. For these doped $LiMnO_2$ at the same doping concentration, Cr-doping shows the highest discharge capacity and best cycling performance, Al-doping offers the lowest discharge capacity and Co-doping shows the worst cycling performance.

Acknowledgements

This work was supported by the Scientific Research Fund of Hunan Provincial Education Department (No. 07B060) and the Backbone Young Teacher Fund of Hunan Provincial Education Department.

References

Armstrong A R and Bruce P G 1996 *Nature* **381** 499
Captiaine F, Gravereau P and Delmas C 1996 *Solid State Ionics* **89** 197
Ceder G and Mishra S K 1999 *Electrochem. Solid State Lett.* **2** 550
Eriksson T A and Doeff M M 2003 *J. Power Sources* **119** 145
Guo Z P, Wang G X, Liu H K and Dou S X 2002 *Solid State Ionics* **148** 359
Gu Y, Zhou H and Chang W 2004 *Rare Metal Mat. Eng.* **33** 789
Hwang S J, Park H S and Choy J H 2002 *Solid State Ionics* **151** 275
Julien C M, Banov B, Momchilov A and Zaghib K 2006 *J. Power Sources* **159** 1365
Kim J U, Jo Y J, Park G C, Jeong W J and Gu H B 2003 *J. Power Sources* **119** 686
Lee Y S, Sun Y K, Adachi K and Yoshio M 2003 *Electrochim. Acta* **48** 1031
Myung S T, Komaba S, Hirosaki N, Kumagai N, Arai K, Kodama R, Terada Y and Nakai I 2003 *J. Power Sources* **119–121** 211
Myung S T, Komaba S, Kurihara K and Kumagai N 2006 *Solid State Ionics* **177** 733
Park K S, Cho M H, Jin S J, Nahm K S and Hong Y S 2004 *Solid State Ionics* **17** 141